



ELSEVIER

Surface Science 327 (1995) 38–46

surface science

# Influence of alloyed Sn atoms on the chemisorption properties of Ni(111) as probed by RAIRS and TPD studies of CO adsorption

Chen Xu, Bruce E. Koel \*

*Department of Chemistry, University of Southern California, Los Angeles, CA 90089-0482, USA*

Received 1 June 1994; accepted for publication 21 November 1994

## Abstract

The chemisorption of CO on Ni–Sn alloys formed on a Ni(111) surface has been studied with reflection–absorption infrared spectroscopy (RAIRS) and temperature programmed desorption (TPD). Formation of the  $(\sqrt{3} \times \sqrt{3})R30^\circ$ -Sn/Ni(111) surface alloy strongly suppresses CO adsorption. Only 0.04 ML CO can be chemisorbed on this surface at 110 K, exclusively at atop sites. The binding energy of this adsorbed CO is reduced to only about 15 kcal/mol. Additionally, no significant effect of subsurface Sn on CO chemisorption on this alloy was observed. These results are in sharp contrast to our previous results for CO chemisorption on the  $(\sqrt{3} \times \sqrt{3})R30^\circ$ -Sn/Pt(111) surface alloy, where the chemisorbed CO saturation coverage, adsorption site distribution and desorption temperature were quite similar to those properties of the Pt(111) surface. We ascribe the influence of alloyed Sn atoms on the CO chemisorption properties of this Sn/Ni(111) surface alloy to be due to repulsive Sn–CO interactions at the Ni–CO distance required for chemisorption. The differences in the chemisorption properties of these Pt–Sn and Ni–Sn alloys are rationalized by considering the different sizes of the surface unit cells and the location of Sn with respect to the surface plane (the Sn buckling distance). These results have important implications for the discussion and determination of ensemble sizes at bimetallic surfaces since the surface chemistry depends strongly on the vertical position of the modifier.

**Keywords:** Alloys; Carbon monoxide; Chemisorption; Infrared absorption spectroscopy; Low index single crystal surfaces; Nickel; Thermal desorption spectroscopy; Tin

## 1. Introduction

The chemistry and catalysis of bimetallic surfaces are strongly modified from that of their single-component constituents [1]. This fact has motivated intensive studies in the past to search for new catalysts and to provide a fundamental explanation for these altered properties [2,3]. The presence of a second component at a bimetallic surface can alter the chem-

istry of the other metal component in two primary ways: (i) electronic effects, whereby the electronic structure at an adjacent site is modified, or (ii) geometric effects, whereby the modifier acts simply as a site-blocker to directly reduce the size and number of reactive sites (ensembles) on the surface. Distinguishing experimentally between electronic and geometric effects remains a very difficult but important task. Ordered surface alloys are especially useful systems to study in this regard due to their known and stable composition and structure.

Evaporation of Sn onto transition metals such as

\* Corresponding author. Fax: +1 213 746 4945. E-mail: koel@chem1.usc.edu.

Ni, Pd, Pt, Rh, Ru and Cu, and subsequent annealing can produce well-ordered surface alloys [3–9]. These surface alloys are often very stable and comprised of a single layer of the alloy on top of the substrate. In several cases it has been found that Sn atoms are almost coplanar with the substrate surface atoms, with some outward buckling of Sn atoms. The magnitude of the buckling has been correlated to the lattice mismatch of Sn with the substrate [5]. The buckling for Sn/Pt(111) is about 0.022 nm [4], while the buckling for Sn/Ni(111) is about 0.046 nm [5,6]. Previously, we have systematically studied the adsorption behavior of Sn/Pt(111) surface alloys [10–16]. It is interesting to now compare the chemisorption properties of Sn/Ni(111) and Sn/Pt(111) surface alloys and to address the influence of the magnitude of Sn buckling on the chemistry of these bimetallic surfaces.

Herein we report on CO adsorption studies designed to probe the surface chemistry. The adsorption of CO on Ni(111) has been intensively studied in the past with many surface science techniques [17–23]. However, some new information is still forthcoming regarding this system. For instance, CO adsorption was originally assigned to the bridge-site at 0.5 ML using high resolution electron energy loss spectroscopy (HREELS), which shows a single  $\nu_{\text{CO}}$  vibrational peak at  $1905\text{ cm}^{-1}$  [17,20,21]. But, a recent surface-extended X-ray-absorption fine-structure (SEXAFS) study [24] shows that CO occupies threefold hollow sites at 0.5 ML CO coverage. The formation of the  $(\sqrt{3} \times \sqrt{3})\text{R}30^\circ\text{-Sn/Ni(111)}$  surface alloy completely removes the threefold-Ni hollow site. Therefore, our experiments also allow us to determine whether CO still adsorbs in this site, even though one of the Ni atoms is replaced by Sn. Briefly, we find that CO chemisorption is strongly suppressed because of the removal of the threefold-Ni hollow site. Furthermore, even the twofold-Ni bridge sites are blocked and CO chemisorbs only on Ni atop sites on the  $(\sqrt{3} \times \sqrt{3})\text{R}30^\circ\text{-Sn/Ni(111)}$  surface alloy.

## 2. Experimental section

The experiments were carried out in a two-stage ultrahigh vacuum chamber equipped with a

quadrupole mass spectrometer (QMS) and optics for low energy electron diffraction (LEED), Auger electron spectroscopy (AES), and reflection-absorption infrared spectroscopy (RAIRS). The top stage is used for RAIRS studies and has a volume of 0.3 L and two  $\text{CaF}_2$  windows to transmit infrared light. This stage also has a sputter ion gun and ion gauge and can be separated from the main chamber with a gate valve for performing high pressure studies. The main chamber is pumped with an ion pump and a turbo-pump with a base pressure of  $1 \times 10^{-10}$  Torr.

The RAIRS spectra were taken by using a Mattson Galaxy 6020 Fourier-transform infrared (FTIR) spectrometer with a MCT detector. A typical spectrum was obtained by signal averaging 1000 scans in a 4 min period with a resolution of  $4\text{ cm}^{-1}$ .

The  $(\sqrt{3} \times \sqrt{3})\text{R}30^\circ\text{-Sn/Ni(111)}$  surface alloys were prepared by evaporating Sn onto a Ni(111) surface and subsequently annealing the sample to 1000 K. It has been shown previously that this

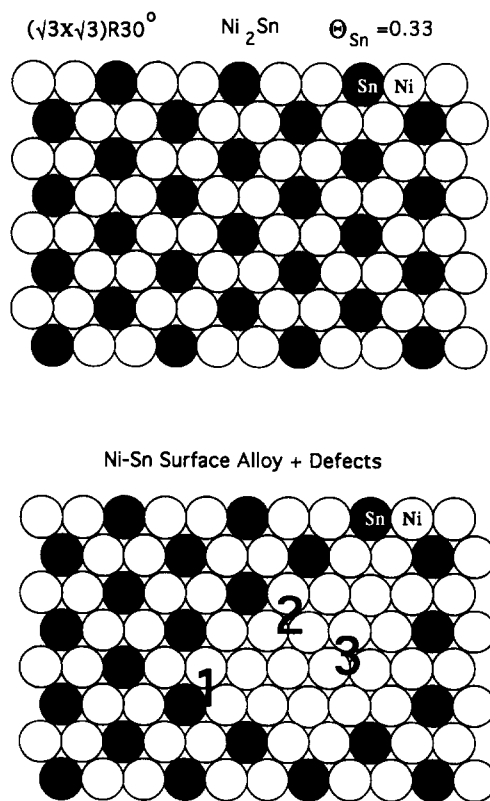


Fig. 1. Structures for the  $(\sqrt{3} \times \sqrt{3})\text{R}30^\circ\text{-Sn/Ni(111)}$  surface alloy.

annealing has no effect on the Sn AES intensity for an initial Sn coverage less than 0.33 ML, while annealing a surface precovered with 0.33–1.0 ML Sn always reduces the Sn AES intensity to the same value corresponding to 0.33 ML [6]. This break point has been used to calibrate the Sn coverage. Two different Sn/Ni(111) surface alloys have been prepared for use in our experiments. The first one was prepared by evaporating about 0.8 ML Sn onto the Ni(111) surface and subsequently annealing at 1000 K for 1 min. The second one was produced by evaporating 0.3 ML Sn onto the surface and annealing to 1000 K for 1 min. After annealing, the Sn coverage on this latter surface corresponded to  $\approx 0.29$  ML in AES. The second surface, therefore, has a Sn deficiency of  $\approx 0.04$  ML compared to the first one. Both surfaces show a very good and visually identical  $(\sqrt{3} \times \sqrt{3})R30^\circ$  LEED pattern. For brevity, the first surface will be referred to as the  $\sqrt{3}$  surface alloy, as derived from the alkali ion scattering spectroscopy (ALISS) studies of Ku and Overbury [6], and the second one as the “defective”  $\sqrt{3}$  surface alloy. A schematic drawing of the  $\sqrt{3}$  surface alloy is provided in Fig. 1a. In Fig. 1b, a possible structure for the defective  $\sqrt{3}$  surface alloy is also provided. On this surface we distinguish between three different threefold hollow ensembles in Ni-rich patches: site 1 comprised of both Sn and Ni atoms, site 2 which contains only Ni atoms but has Sn atoms as nearest-neighbors, and site 3 which contains no Sn atom nor has Sn atoms as nearest-neighbors.

### 3. Results

#### 3.1. CO chemisorption on $(\sqrt{3} \times \sqrt{3})R30^\circ$ -Sn/Ni(111) surface alloys

A series of TPD spectra for increasing CO exposures are shown in Fig. 2. A single desorption peak was observed at 253 K independent of CO coverage. At high CO exposures, a high temperature tail near 280 K begins to develop, but this is probably due to desorption from the sample holder or crystal edges and back (see below). AES spectra taken after TPD experiments show a clean surface without any trace

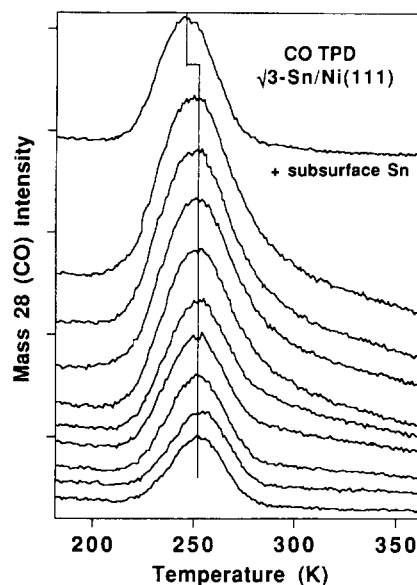


Fig. 2. CO TPD on the  $\sqrt{3}$  Sn/Ni(111) surface alloy.

of carbon or oxygen, indicating completely reversible adsorption of CO on the  $\sqrt{3}$  surface alloy. Using the well-known CO coverage of 0.5 ML on clean Ni(111) at 300 K [21] and the TPD areas, we can determine that the saturation coverage of CO on the  $\sqrt{3}$  surface alloy is 0.04 ML, only 9% of the saturation coverage of CO on clean Ni(111). *The ability of Ni(111) to chemisorb CO is strongly reduced by the presence of 0.33 ML Sn alloyed in the surface layer.* Another influence of Sn is indicated by the strong reduction of the CO desorption temperature. On Ni(111), CO desorbs principally in a peak at 430 K. Using Redhead analysis [25], the change in the CO desorption temperature corresponds to a binding energy decrease of 11.4 kcal/mol. These results can be contrasted to those obtained on the  $(\sqrt{3} \times \sqrt{3})R30^\circ$ -Sn/Pt(111) surface alloy. Both the saturation coverage and binding energy of CO is only slightly reduced on the  $\sqrt{3}$  Sn/Pt(111) surface alloy compared to Pt(111) [10].

As mentioned above, the  $\sqrt{3}$  surface alloy produced using the procedure described in the experimental section is a true surface alloy and comprises only a single Sn-containing layer [5,6]. No subsurface Sn was detected using ALISS [5,6]. However, if one evaporates more than 1 ML Sn onto the surface and anneals to 1000 K, substantial subsurface Sn can

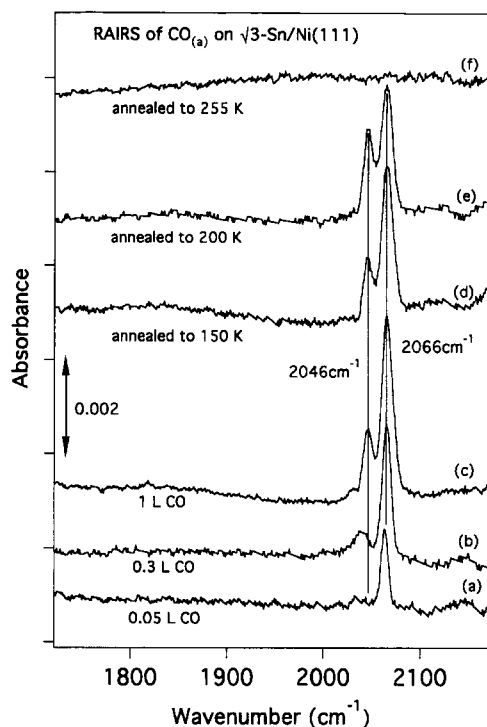


Fig. 3. RAIRS of CO on the  $\sqrt{3}$  Sn/Ni(111) surface alloy.

be detected using ALISS [5,6]. The first layer structure remains the same in both cases [6]. Therefore, it is interesting to address the influence of subsurface Sn on the adsorption behavior of CO. To produce the  $\sqrt{3}$  surface alloy with subsurface Sn, we evaporated 3 layers of Sn on Ni(111) and then annealed the surface to 1000 K. LEED shows a sharp ( $\sqrt{3} \times \sqrt{3}$ )R30° pattern and AES measurements show an increased Sn AES signal compared to 0.33 ML. TPD spectra taken after saturation CO exposures on this surface show desorption traces very similar to the  $\sqrt{3}$  surface alloy, but with a temperature shift to lower desorption temperature by about 10 K. This indicates only a small influence of subsurface Sn on CO adsorption. Since the influence of subsurface Sn can only be electronic in nature, this result is consistent with a small electronic effect of Sn on CO adsorption on Ni(111).

CO adsorption on the  $\sqrt{3}$  surface alloy has also been studied with RAIRS. Fig. 3 shows a series of RAIRS spectra for different conditions. The spectra for curves (a)–(c) were taken after increasing CO

exposure at 120 K. Only vibrational modes above  $2000 \text{ cm}^{-1}$  were observed on this  $\sqrt{3}$  surface alloy. Thus, no CO was adsorbed on twofold bridge or threefold hollow sites. CO only adsorbs on the  $\sqrt{3}$  surface alloy at atop sites. However, we did observe two peaks at 2046 and 2066  $\text{cm}^{-1}$ . Both peaks are very sharp ( $\text{FWHM} = 12 \text{ cm}^{-1}$ ) and their position is independent of the CO coverage. An annealing series is also shown in Fig. 3, as curves (c)–(f). Annealing to 150 K does not cause a significant change in the RAIRS spectra. Annealing to 200 K causes a small drop in the intensity of the high frequency peak and a slight increase in the size of the low frequency peak. Increasing the annealing temperature further to 255 K completely desorbs CO from the surface. This is in good agreement with the TPD results showing that CO desorbs in a single peak at 253 K. Two RAIRS peaks were always observed independent of the initial Sn coverage (varying from 0.4 to 3 ML). However, the relative intensity of the two peaks varies with the preparation conditions (initial Sn coverage and annealing time at 1000 K).

### 3.2. CO chemisorption on a defective $\sqrt{3}$ -Sn/Ni(111) alloy

Since the adsorption of CO on the  $\sqrt{3}$  surface alloy is so strongly suppressed, we also studied the adsorption of CO on defective surface alloys which had a surface Sn concentration of only about 0.29 ML. Nonetheless, a sharp ( $\sqrt{3} \times \sqrt{3}$ )R30° LEED pattern was also observed for these defective surface alloys. TPD spectra after increasing CO exposures on the defective surface alloy are shown in Fig. 4. A small CO background curve (taken with the surface covered with five layers of Sn) is subtracted from all of the spectra. At small CO coverages, we first see a desorption peak at 423 K. With increasing CO exposures, two peaks at 251 and 310 K also form. Assuming first-order desorption kinetics and a pre-exponential factor of  $1 \times 10^{-13}$ , Redhead analysis can be used to convert these two desorption temperatures to binding energies of 15 and 19 kcal/mol, respectively.

In Fig. 5, we directly compare the CO TPD spectra for saturated coverages of CO on a defective surface alloy with that from the  $\sqrt{3}$  surface alloy and Ni(111). CO TPD spectra from Ni(111) surfaces is

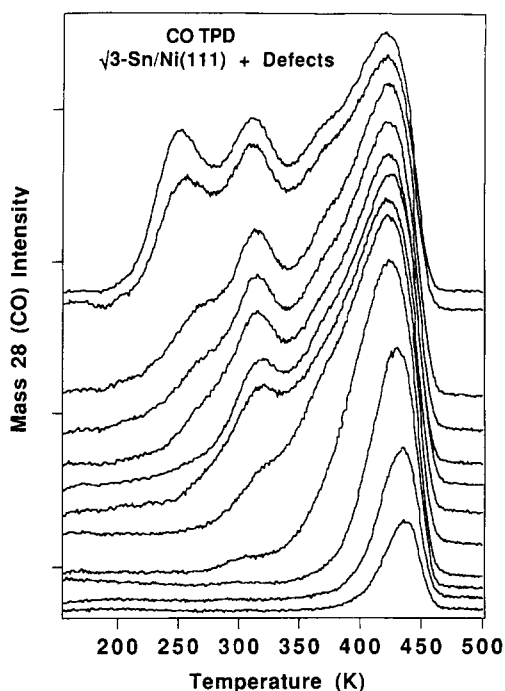


Fig. 4. CO TPD on a defective surface alloy.

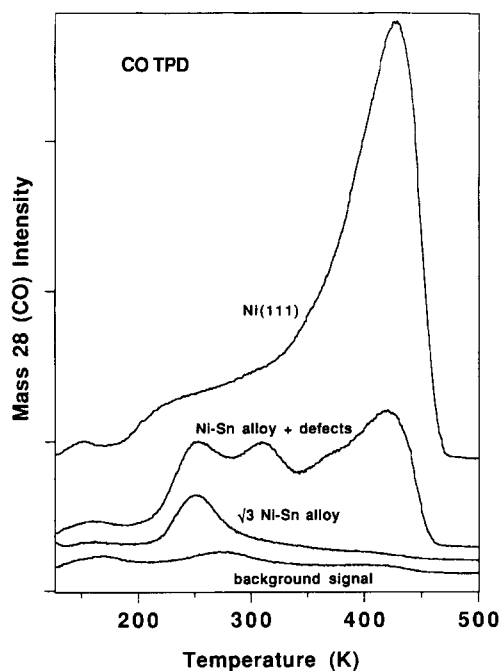


Fig. 5. Comparison of CO TPD on Ni(111),  $\sqrt{3}$  surface alloy and a defective surface alloy.

dominated by a large peak at 428 K. A broad shoulder at lower desorption temperatures is also seen, which arises from repulsive CO–CO interactions in the so-called “compressed CO layer” at high CO coverages. Comparing the curve for Ni(111) to that from the defective surface alloy, the desorption temperature of the dominant peak at 428 K only shifts slightly to 423 K. The intensity of this peak, however, is reduced by a factor of three with the presence of 0.29 ML Sn in the surface layer. At the expense of intensity in this peak, two clearly identifiable peaks at lower desorption temperature appear. The peak at 423 K can be correlated to Ni(111)-like sites. By comparison to the curve from the  $\sqrt{3}$  surface alloy the peak at 251 K is attributed to the desorption of CO on the regular sites of the  $\sqrt{3}$  surface alloy. The peak at 310 K is therefore related to sites characteristic of the defective surface alloy. Since both the  $\sqrt{3}$  surface alloy sites and Ni(111)-like sites show almost identical desorption temperatures as their respective, defect-free surfaces, the defects exert only a very local influence on the surface chemistry. From the coverage calculated from the TPD areas and the amount of Ni-rich patches estimated from AES, we believe that the desorption peak at 310 K is due to CO adsorbed on site 1 ensembles and the peak at 423 K is due to ensembles like sites 2 and 3 (these sites are shown in Fig. 1). This assignment is also consistent with the CO desorption temperature change that occurs in comparing clean Ni(111) to the defective  $\sqrt{3}$  surface alloy and from the defective  $\sqrt{3}$  surface alloy to the  $\sqrt{3}$  surface alloy. The same effect which caused a strong decrease in the CO desorption temperature on the  $\sqrt{3}$  surface alloy also produces the desorption peak at 310 K on the defective surface alloy. From these results we can conclude that the strong influence of Sn on CO adsorption on Ni(111) is mostly due to a short-range interaction between Sn and CO rather than a long-range electronic effect.

Fig. 6 shows the CO uptake curve that is obtained by plotting the CO TPD areas versus the CO exposures on Ni(111) and the defective  $\sqrt{3}$  surface alloy. The saturation coverage of CO on the defective  $\sqrt{3}$  surface alloy is reduced to about 0.23 ML. By contrast, the initial sticking coefficient given by the initial slope of the uptake curves is decreased only slightly in comparison to the Ni(111) surface. This

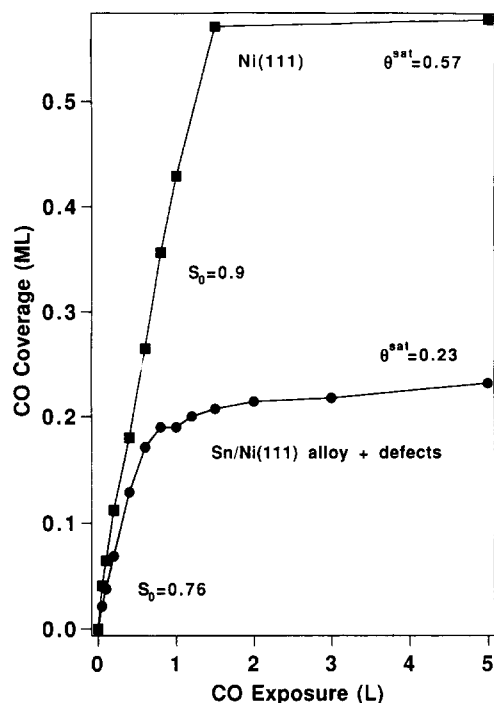


Fig. 6. CO uptake on a defective surface alloy.

result is due to the important presence of the so-called “modifier precursor” CO state on top of Sn atoms which prevents a linear decrease of the initial sticking coefficient with increasing Sn concentration in the surface layer [26].

The adsorption of CO on the defective  $\sqrt{3}$  surface alloy has also been studied with RAIRS. In Fig. 7 we compare the RAIRS spectra obtained after saturation CO exposures on Ni(111), the  $\sqrt{3}$  surface alloy, and a defective  $\sqrt{3}$  surface alloy. The RAIRS spectrum of CO on a defective  $\sqrt{3}$  surface alloy is characterized by the presence of two broad peaks at 1880 and 2070  $\text{cm}^{-1}$ . The peak at 2070  $\text{cm}^{-1}$  can be assigned to CO adsorbed at atop sites, while the peak at 1880  $\text{cm}^{-1}$  can be assigned either to twofold bridge or threefold-hollow sites. These two peaks show a very different temperature dependence, which is shown in Fig. 8. The spectra in Fig. 8A were taken after dosing 0.2 L CO onto the surface at 120 K and subsequently heating to the indicated temperature. At this low CO coverage ( $\sim 0.05$  ML), two peaks are seen at higher frequencies (2048 and 2068  $\text{cm}^{-1}$ ) and the peak at lower frequency appears near 1810

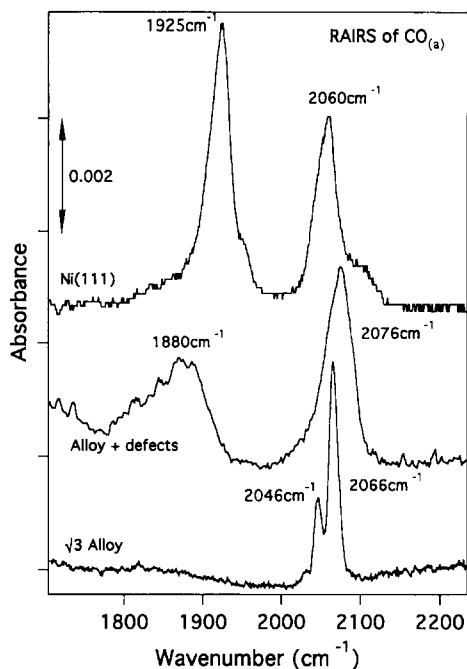


Fig. 7. Comparison of RAIRS of CO on Ni(111),  $\sqrt{3}$  surface alloy and a defective surface alloy.

$\text{cm}^{-1}$ . While some changes occur within each of these features with increasing temperatures, we focus here on a comparison of the two regions. At lower temperatures, both regions have similar intensities. Increasing the surface temperature causes a conversion of the intensity of the high frequency peaks to the lower frequency peak. At 300 K, the peaks above

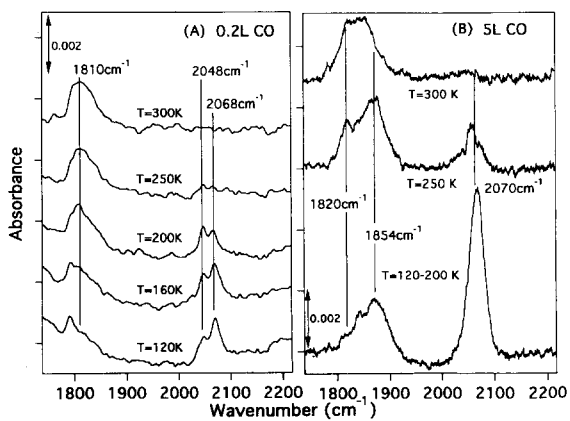


Fig. 8. Temperature effects on RAIRS of CO on a defective surface alloy.

2000  $\text{cm}^{-1}$  disappear completely. This conversion is irreversible. Lowering the surface temperature does not repopulate the high frequency peaks. The conclusion that CO adsorbed on atop sites is converted to CO adsorbed on bridge or threefold hollow sites that is indicated by these results is also supported by the TPD results which shows no CO desorption below 300 K at a CO exposure of 0.2 L. Fig. 8B shows that a saturation exposure of CO at 300 K can not populate states with CO modes above 2000  $\text{cm}^{-1}$  either. This demonstrates that CO bonded on atop sites has a much smaller binding energy compared to CO bonded on twofold bridge or threefold hollow sites. The adsorption of CO at atop sites at lower temperature and lower coverage is due to a kinetic effect which prevents the diffusion of CO from atop sites on the alloy phase regions to bridge sites at defects which have low Sn concentrations. These results can be contrasted with those for CO adsorption on the clean Ni(111) surface where the conversion between CO adsorbed on atop and bridge sites is completely reversible, the population ratio of the two sites is only determined by the temperature, and the binding energy of CO on these two sites is very similar [20].

#### 4. Discussion

The most surprising result that emerged from these experiments was the strong suppression of CO chemisorption on the  $\sqrt{3}$  surface alloy. Both the CO desorption temperature and saturation coverage are dramatically changed. This is surprising based on our previous studies of CO adsorption on Sn/Pt(111) surface alloys in which we found that the CO saturation coverage and desorption temperature of CO on the  $(\sqrt{3} \times \sqrt{3})\text{R}30^\circ\text{-Sn/Pt(111)}$  surface alloy are very similar to the Pt(111) surface [10]. Both Pt(111) and Ni(111) form a well-ordered  $(\sqrt{3} \times \sqrt{3})\text{R}30^\circ$  surface alloy with 0.33 ML Sn based on ALISS measurements [4,6]. In both cases, Sn is incorporated into the substrate surface layer; however, Sn protrudes only 0.022 nm above the surface for Sn/Pt(111) but 0.046 nm for Sn/Ni(111) [4,6]. How can we understand the dramatic difference between the Ni–Sn and Pt–Sn alloys?

Table 1  
Properties of Sn, Pt, and Ni relevant to bonding in Pt–Sn and Ni–Sn alloys

	Work function $\phi$ (eV)	Electronegativity, $\chi$		Alloy heat of formation $\Delta H_f^0$ (kcal/mol)
		Pauling	Allred-Rochow	
Sn	4.42 <sup>a</sup>	1.8	1.72	
Pt	5.7 <sup>b</sup>	2.2	1.44	–12 <sup>d</sup>
Ni	5.35 <sup>c</sup>	1.9	1.75	–5.6 <sup>c</sup>

<sup>a</sup> Sn(poly) [28]; <sup>b</sup> Pt(111) [28]; <sup>c</sup> Ni(111) [28]; <sup>d</sup> Pt<sub>3</sub>Sn [29]; <sup>e</sup> Ni<sub>3</sub>Sn [30].

A key question to be answered certainly concerns whether the change in CO adsorption on Ni(111) from alloying is due to an electronic or geometric effect. Both our intuition and experimental results indicate that it is a primarily a geometric or site-blocking effect due to repulsive interactions between Sn and CO. In Table 1 we list the electronegativities of Sn, Ni, and Pt according to Pauling and Allred-Rochow. The work function of Sn(poly), Ni(111) and Pt(111) and heats of formation of Sn–Ni and Sn–Pt alloys are also given. The electronegativity and work function of Sn are much closer to Ni(111) than to Pt(111). One would expect, therefore, a smaller electronic modification of the Ni(111) surface by alloyed Sn than of the Pt(111) surface. From previous investigations we know that alloyed Sn has a very small electronic effect on CO adsorption on Pt(111) [10], and therefore, we would also expect a negligible electronic effect of alloyed Sn on CO adsorption on Ni(111).

Some experimental results also support this prediction. First, the presence of subsurface Sn, which can affect CO adsorption only through an indirect electronic effect, has little effect on CO adsorption. Secondly, the results on a defective surface alloy show clearly that only CO adsorbed directly on a defect site (site 1) is influenced by the presence of defect sites. By contrast, CO adsorbed on the regular  $\sqrt{3}$  surface alloy sites and on the “clean Ni” sites (sites 2 and 3) are not influenced by the presence of defect sites. Thus, there is only a short range interaction between CO and Sn which causes the strong decrease in the CO desorption temperature.

Within the context of a site-blocking model for explaining the influence of alloyed Sn atoms on CO

adsorption on Ni(111), we present below three possible explanations for the origin of the effect.

#### 4.1. Elimination of adsorption sites

While the adsorption of CO has been extensively studied using various surface science techniques, there are still some new developments regarding the adsorption sites. Previously, the adsorption site at small coverage was assigned based on two HREELS peaks at 1816 and 1831  $\text{cm}^{-1}$  to the threefold and twofold bridging sites, respectively [17,21]. At higher coverages, the HREELS spectra are dominated by two peaks at about 2050 and 1900  $\text{cm}^{-1}$  which were correlated to CO adsorbed at atop and twofold bridge sites, respectively. A single peak at 1905  $\text{cm}^{-1}$  appears at a CO coverage of 0.5 ML which gives a sharp  $c(4 \times 2)$  LEED pattern [21]. This CO species was also assigned to the twofold bridge site. However, a recent SEXAFS and LEED study reassigned this species to CO adsorbed in the three-fold hollow site [24]. On the  $\sqrt{3}$  Ni–Sn surface alloy, there are no threefold hollow sites containing only Ni atoms. Therefore, CO adsorption on three-fold Ni hollow sites is eliminated. Now, the adsorption of CO on twofold bridge sites must be very energetically unfavorable since there are plenty of the twofold Ni bridge sites present on the  $\sqrt{3}$  surface alloy but CO only adsorbs at atop sites. This explanation is not completely satisfactory since it implies that the adsorption of CO is *very* site-specific, and a question also remains as to why the binding energy of CO adsorbed at atop sites is reduced by more than 11 kcal/mol if no large electronic modification of the Ni surface exists.

#### 4.2. Repulsive interaction between Sn and CO

Supplementary to the explanation just presented above, if there are additional direct Sn–CO interactions we can explain our results in a very satisfactory manner. Since CO does not adsorb onto Sn surfaces at temperatures exceeding 90 K, the interaction between Sn and CO is comprised mainly of weak Van der Waals forces. If the distance between Sn and CO is smaller than the sum of their Van der Waals radii, some repulsive interactions will be present. Since Sn

has a larger outward buckling on Sn/Ni(111) (0.046 nm) than on Sn/Pt(111) (0.022 nm) and Ni(111) has a smaller distance between adjacent Ni(111) atoms (0.249 nm) than Pt(111) does (0.277), the distance between the carbon atom of chemisorbed CO (bound to either Ni or Pt) and the Sn surface atom will be smaller on the Sn/Ni(111) surface alloy than on the Sn/Pt(111) surface alloy. This smaller distance can cause a substantial repulsive interaction between CO and Sn. Since the distance between a CO molecule adsorbed at a twofold Ni bridge site and a Sn atom is smaller than that between CO at an atop site and Sn, adsorption of CO on twofold Ni bridge sites could be eliminated. Adsorption of CO on atop sites is still possible, but with a much smaller binding energy because of the repulsive interactions of adsorbed CO with three adjacent Sn atoms. This argument illustrates that the influence of a modifier on the surface chemistry depends strongly on the vertical position of the modifier. *Efforts to determine ensemble sizes based on the influence of site-blockers should consider this effect.*

Another question remains concerning why the coverage of atop-site CO on the  $\sqrt{3}$  surface alloy is so small, i.e., only 0.04 ML (9% of saturation coverage on Ni(111)). One possible explanation is that three adjacent Sn atoms are displaced laterally due to the repulsive interaction of CO and Sn (or possibly due to CO-induced changes in the Ni electronic structure), causing the atop sites adjacent to these Sn atoms to not be available for CO adsorption. This would strongly reduce the CO saturation coverage. This explanation is supported by the much smaller vibrational linewidth of CO adsorbed on the  $\sqrt{3}$  surface alloy compared to that on Ni(111). CO molecules adsorbed on the  $\sqrt{3}$  surface alloy are obviously well-separated and the broadening due to short range CO–CO (repulsive) interactions is therefore limited.

#### 4.3. Surface structure

Another possible explanation, which we deem to not be very likely, is that the structural determination of the Sn/Ni(111) surface alloy was incorrect. This would mean that the  $(\sqrt{3} \times \sqrt{3})R30^\circ$ -Sn/Ni(111) surface alloy has a totally different structure than the

$(\sqrt{3} \times \sqrt{3})R30^\circ$ -Sn/Pt(111) surface alloy. For instance, the Sn coverage on the  $(\sqrt{3} \times \sqrt{3})R30^\circ$ -Sn/Ni(111) could be 0.67 ML instead of 0.33 ML, as it is for the Sn/Ru(001) surface alloy [9]. Both surface nets give the same LEED patterns. It is also possible that the Sn atoms are present as an overlayer on Ni(111). This would certainly block CO adsorption more effectively. However, considering that the same annealing temperature (1000 K) was used to produce the Sn/Ni(111) and Sn/Pt(111) structures, this is not very likely either. In any case, a reexamination and verification of the structure of the  $(\sqrt{3} \times \sqrt{3})R30^\circ$ -Sn/Ni(111) surface alloy using other independent techniques would be helpful. For instance, the structure determined by ALISS for the Sn/Pt(111) surface alloy has been reexamined and verified using dynamic LEED measurements [27].

### Acknowledgments

This work was partially supported by the Division of Chemical Sciences, Office of Basic Energy Sciences, U.S. Department of Energy. Instrumentation used in this work was partially supported by the Army Research Office under the auspices of the URI Center for Studies of Fast Transient Processes. The authors would like to thank Dr. Mike Bartram and Dr. Randy Creighton for their advice concerning the instrumentation for FTIR spectroscopy and especially to acknowledge the contribution of Dr. Peter Blass in constructing the hardware used in this experiment.

### References

- [1] J.H. Sinfelt, *Bimetallic Catalysis: Discoveries, Concepts, and Applications* (Wiley, New York, 1983).
- [2] C.T. Campbell, *Ann. Rev. Phys. Chem.* 41 (1990) 775.
- [3] M.T. Paffett and R.G. Windham, *Surf. Sci.* 208 (1989) 34.
- [4] S.H. Overbury, D.R. Mullins, M.T. Paffett and B.E. Koel, *Surf. Sci.* 254 (1991) 45.
- [5] S.H. Overbury and Y.-S. Ku, *Phys. Rev. B* 46 (1992) 7868.
- [6] Y.-S. Ku and S.H. Overbury, *Surf. Sci.* 273 (1992) 341.
- [7] M.T. Paffett, A.D. Logan, R.J. Simonson and B.E. Koel, *Surf. Sci.* 250 (1991) 123.
- [8] M.T. Paffett and A.D. Logan, in: *New Frontiers in Catalysis, Proc. 10th Int. Conf. Catal., Budapest, Hungary, July 1992*, p. 1595.
- [9] M.T. Paffett, A.D. Logan and T.N. Taylor, *J. Phys. Chem.* 97 (1993) 690.
- [10] M.T. Paffett, S.C. Gebhard, R.G. Windham and B.E. Koel, *J. Phys. Chem.* 94 (1990) 6831.
- [11] M.T. Paffett, S.C. Gebhard, R.G. Windham and B.E. Koel, *Surf. Sci.* 223 (1989) 449.
- [12] C. Xu, J.W. Peck and B.E. Koel, *J. Am. Chem. Soc.* 115 (1993) 751.
- [13] C. Xu and B.E. Koel, *Langmuir* 10 (1994) 166.
- [14] C. Xu and B.E. Koel, *Surf. Sci.* 304 (1994) 249.
- [15] C. Xu and B.E. Koel, *Surf. Sci.* 304 (1994) L505.
- [16] C. Xu, L. Tsai and B.E. Koel, *J. Phys. Chem.* 98 (1994) 585.
- [17] W. Erley, H. Wagner and H. Ibach, *Surf. Sci.* 80 (1979) 612.
- [18] M. Trenary, K.J. Uram, F. Bozso and J.T. Yates, Jr., *Surf. Sci.* 146 (1984) 269.
- [19] B.N.J. Persson and R. Ryberg, *Phys. Rev. Lett.* 54 (1985) 2119.
- [20] S.L. Tang, M.B. Lee, Q.Y. Yang, J.D. Beckerle and S.T. Ceyer, *J. Chem. Phys.* 84 (1986) 1876.
- [21] L. Surnev, Z. Xu and J.T. Yates, Jr., *Surf. Sci.* 201 (1988) 1.
- [22] L. Surnev, Z. Xu and J.T. Yates, Jr., *Surf. Sci.* 201 (1988) 14.
- [23] L.S. Caputi, R.G. Agostino, A. Amoddeo, S. Molinaro, G. Chiarello, E. Colavita and A. Santaniello, *Surf. Sci.* 289 (1993) L591.
- [24] L. Becker, S. Aminpirooz, B. Hillert, M. Pedio, J. Haase and D.L. Adams, *Phys. Rev. B* 47 (1993) 9710.
- [25] P. Redhead, *Vacuum* 12 (1962) 203.
- [26] C. Xu and B.E. Koel, *J. Chem. Phys.* 100 (1994) 664.
- [27] A. Atrei, U. Bardi, J.X. Wu, E. Zanazzi and G. Rovida, *Surf. Sci.* 290 (1993) 286.
- [28] H.B. Michaelson, *J. Appl. Phys.* 48 (1977) 4731.
- [29] R. Ferro, R. Capelli, A. Borsese and S. Delfino, *Lincei-Rend. Sci. Fis. Mater. E Nat.* 54 (1973) 634.
- [30] R. Hultgern, P.D. Desai, D.T. Hawkins, M. Gleiser and K.K. Kelley, *Selected Values of Thermodynamic Properties of Binary Alloys* (American Society for Metals, OH, 1973).